Sensors and Actuators B 220 (2015) 1033–1042

Contents lists available at ScienceDirect

Sensors and Actuators B: Chemical

journal homepage: www.elsevier.com/locate/snb

A single-loop fiber attenuated total reflection sensor enhanced by silver nanoparticles for continuous glucose monitoring

Dachao Li[a,*], Yanwen Sun[b], Songlin Yu[c], Changyue Sun[b], Haixia Yu[b], Kexin Xu[a]

[a] State Key Laboratory of Precision Measuring Technology and Instruments, Tianjin University, China
[b] Tianjin Key Laboratory of Biomedical Detecting Techniques and Instruments, Tianjin University, China
[c] Tianjin Institute of Metrological Supervision Testing, Tianjin, China

ARTICLE INFO

Article history:
Received 30 January 2015
Received in revised form 17 April 2015
Accepted 11 June 2015
Available online 20 June 2015

Keywords:
Continuous glucose monitoring
Fiber ATR sensors
Single-loop structure
Silver nanoparticles
Surface enhanced IR absorption

ABSTRACT

Currently, the implantable enzyme electrode sensor is the only method for continuous glucose monitoring in clinical applications, but the significant drift caused by bioelectricity in body and the effect of electrochemical reactions under hypoxia reduce the accuracy of the glucose measurements. Therefore, finger-prick blood corrections are often required to calibrate enzyme-based glucose sensors several times each day. In this paper, we proposed an implantable miniaturized fiber Attenuated Total Reflection (ATR) sensor based on mid-infrared spectroscopy to overcome the two drawbacks. A single-loop structure of fiber ATR sensor was used to increase the effective optical length to enhance the sensitivity. By growing silver nanoparticles (AgNPs) on the cylindrical surface of the fiber ATR sensor with a chemical silver mirror method, the sensitivity of the infrared absorption signal was further enhanced. In the experiment, the fiber ATR sensor enhanced by AgNPs combined with a CO_2 laser showed an intense absorption signal from glucose, with enhancement factors of two to six folds at different absorption wavenumbers compared with the bare fiber ATR sensors. The prediction of glucose concentration with high accuracy was achieved by using the five-variable partial least-squares model yielding a root-mean-square error of prediction as small as 4.45 mg/dL.

1. Introduction

Diabetes mellitus is a common chronic disease that requires to monitor blood glucose level continuously to provide guidance for diagnosis and therapy [1–3]. Today the only method in clinic for continuous glucose determination is the enzyme electrode sensing technique, which is realized by measuring the enzyme reaction electricity while the enzyme electrode is implanted in subcutaneous tissue. Some representative produ cts based on this technique include SEVEN® Plus (DexCom, Inc.) [4], Paradigm® REAL-Time (Medtronic, Inc.) [5,6], FreeStyle Navigator® (Abbott Laboratories) [7], etc. However, two problems of the enzyme electrode sensing technique need to be paid close attention: (1) The glucose concentration is determined by measuring the current generated by the enzymatic reactions when used with the enzyme electrode sensor. However, the change of potential in the biological processes caused by electrochemical reactions under hypoxia in the body which is called bioelectricity, leads to significant signal drift and reduces the glucose concentration measurement accuracy, especially for a long period of continuous glucose monitoring. Consequently, it is necessary to take frequent finger prick blood for calibration which causes additional pain and inconvenience for the patient [8,9]. (2) The local glucose level is irreversibly depleted by the glucose oxide enzyme, resulting in measurement inaccuracy at low glucose concentrations. Therefore it is more difficult to find hypoglycemia in clinical treatment [10,11]. However, it is very important to monitor hypoglycemia, which is potentially dangerous if not discovered in time.

The fiber-based technique provides an excellent approach to fabricate miniaturized ATR sensors [12,13], which makes it possible to implant the sensor into subcutaneous tissue. Compared with the enzyme electrode sensing technique, it is more suitable for continuous glucose monitoring over long periods based on the two following advantages. First, fiber sensing is based on optical signals and the measurement is not affected by bioelectricity caused by electrochemical reactions in the body; thus, the signal drift would be reduced greatly and result are more accurate [14]. Second, five emission wavenumbers around the glucose absorption peaks were employed for glucose specific determination, as opposed to

* Corresponding author. Room 407, Building 17, Tianjin University, 92 Weijin Road, Tianjin 300072, China. Tel.: +86 22 27403916; fax: +86 22 27406726.
E-mail address: dchli@tju.edu.cn (D. Li).

http://dx.doi.org/10.1016/j.snb.2015.06.028
0925-4005/

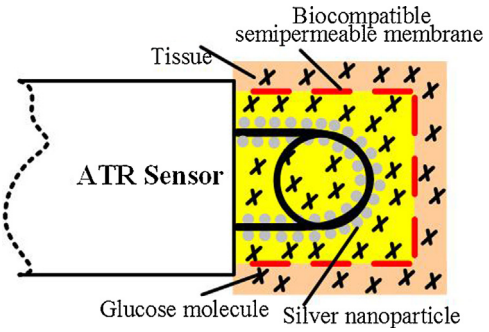

Fig. 1. Schematic diagram of implantable single-loop fiber ATR sensor.

specificity of enzyme [15,16]; thus, no glucose was depleted during the measurement. In this case, hypoglycemia will not be missed, which is very important for continuous glucose monitoring. However, the miniaturization of the fiber ATR sensor could bring about low sensitivity and resolution compared with traditional prism-type ATR sensors. How to improve the sensitivity and measurement resolution of the fiber ATR sensor is the key point for its practical application in continuous glucose monitoring.

In this paper, a single-loop structure of fiber ATR sensor was used to increase the sensing optical length to enhance the sensitivity. Silver has good biocompatibility, and in this paper, we will further improve the sensitivity and measurement resolution of fiber ATR sensor with surface modification by AgNPs on the cylindrical surface of fiber. There are many methods to grow nanoparticles for different applications [17–24]. Vacuum evaporation [17,18] and sputtering [19,20] are two traditional dry process to grow nanoparticles, but these methods are limited on flat substrates and very difficult to apply on a cylindrical surface, especially on the cylindrical surface of a single-loop fiber ATR sensor. Wet chemical processes offers some advantages over dry processes, such as lower cost and easier operation during preparation [21–23]. A reduction method as one type of wet chemical process has been studied to grow AgNPs on flat substrates of silver chloride; Silver ions of the substrate that were dissolved in solution were reduced by agents such as N_2H_4 and $NaBH_4$ in the alkaline condition of sodium hydroxide[22]. Though AgNPs could be grown on the cylindrical surface of the fiber ATR sensor by this reduction method, the surface of fiber might be partly corroded by the sodium hydroxide, which might lead to light leakage and the reduction of the measurement resolution of fiber ATR sensor. In this paper, we grow AgNPs on the cylindrical surface of single-loop fiber ATR sensor by a chemical silver mirror method to enhance the measurement sensitivity. The fiber ATR sensor enhanced by AgNPs was characterized and the experiment results show a strong enhancement compared with the bare fiber ATR sensor. Finally, a multivariable partial least-squares model proved that a root-mean-square error of prediction of multiple wavelengths is more accurate than one wavelength. We also found that the fiber ATR sensor enhanced by AgNPs has better performance than the bare ATR sensor. This work lies a technical foundation for implantable glucose measurement by an optical ATR sensor.

2. Design of fiber ATR sensor

2.1. Structure of implantable fiber ATR sensor

Fig. 1 shows the silver-nanoparticle-enhanced fiber ATR sensor that can be implanted into subcutaneous tissue for continuous glucose determination in interstitial fluid (ISF) [25]. The components of the interstitial fluid are simpler than the blood and many macromolecular substances in the blood have been filtered when the glucose molecules penetrates into the interstitial fluid from blood. A cellulose acetate semi-permeable membrane with a selectable molecular weight cut-off was used as a protective cover to separate the implanted sensor from the tissue, further filter out large biological molecules within the ISF and allow glucose molecules to pass through [26]. The sensor was fabricated in three steps: (1) the single-loop fiber ATR sensor; (2) the fabrication of silver nanoparticles; (3) the biocompatible encapsulation of the sensor.

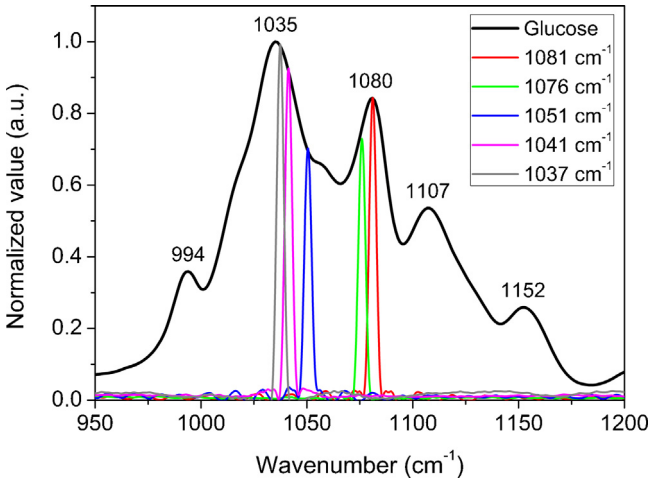

Fig. 2. Normalized laser emission spectrum and absorption spectrum of glucose.

2.2. Specific determination of glucose using tunable laser

The fiber ATR sensor implements the optical measurement based on the mid-IR spectrum of glucose. In our study we used five wavenumbers around the two glucose strong absorption peaks which was emitted by the wavelength tunable CO_2 laser to eliminate or weaken the interference of other compositions in interstitial fluid for the measurement of the glucose concentration [27–29]. Several strong, prominent and isolated glucose absorption peaks in the "finger print" band distinguishes glucose from other interfering species in human blood in vitro [30]. As there are evident absorption peaks of glucose at five different wavenumbers ($994\,cm^{-1}$, $1035\,cm^{-1}$, $1080\,cm^{-1}$, $1107\,cm^{-1}$, $1152\,cm^{-1}$), the wavenumbers emitted by the CO_2 laser was selected over a range of five ($1081\,cm^{-1}$, $1076\,cm^{-1}$, $1051\,cm^{-1}$, $1041\,cm^{-1}$, $1037\,cm^{-1}$) by finely tuning the laser cavity. Furthermore, the five different wavenumbers ($1081\,cm^{-1}$, $1076\,cm^{-1}$, $1051\,cm^{-1}$, $1041\,cm^{-1}$, $1037\,cm^{-1}$), approximating to the two intense absorption peaks of glucose at $1035\,cm^{-1}$ and $1080\,cm^{-1}$. Fig. 2 shows the normalized laser emission spectrum and absorption spectrum of glucose. The optical-based detection does not consume glucose, which is more preponderant than the electrochemical detection. The new method of using five wavenumbers effectively avoids the interferences from other components when measuring the glucose concentration in the interstitial fluid, providing a higher precision and sensitivity.

2.3. Increasement of optical length by single-loop structure

The silver halide polycrystalline infrared fibers are highly transparent in the mid-infrared (mid-IR) range. In addition, they have many desirable properties, such as flexibility, non-toxicity and insolubility in water [31–33], which make them suitable to be implantable ATR sensors. Multimode silver halide polycrystalline infrared fibers with an outer diameter of 700 μm and a core diameter of 630 μm (A.R.T. Photonics GmbH, Berlin, Germany) was used in this paper. The refractive index of the core and cladding were $n_{core} = 2.15$ and $n_{clad} = 2.13$, respectively. To make the implantable

ATR sensors small and highly sensitive, a single-loop structure of ATR sensor was used to reduce the volume but increase the sensing length compared with straight fiber ATR sensor. In this paper, the radius of single-loop fiber ATR sensor was 2.5 mm, which is convenient for the experiment. The size of the single-loop sensor could be further decreased upon implantation. Increasing the effective optical length of fiber-optic ATR sensor would augment the numbers of total reflection, which could directly improve its sensitivity according to Lambert–Beer's law. Therefore, the single-loop fiber ATR sensor is more sensitive than the conventional straight fiber ATR sensor.

2.4. Enhancement of infrared molecules absorption by AgNPs

Silver nanoparticles are grown on the cylindrical surface of a single-loop fiber ATR sensor to achieve the enhancement of the infrared absorption signal as shown in Fig. 1B. The infrared absorption of glucose molecules would be more intense when they were adsorbed on AgNPs than what would be expected from conventional measurements without AgNPs [34]. The intense enhancement was mainly contributed by the electromagnetic and chemical mechanisms. The infrared absorption (A) may be written [34] as (1)

$$A \propto \left|\partial\mu/\partial Q \cdot E\right|^2 = \left|\partial\mu/\partial Q\right|^2 \left|E\right|^2 \cos^2\theta \quad (1)$$

where $\partial\mu/\partial Q$ is the derivative of the dipole moment with respect to a normal coordinate Q, E is the electric field that excites the silver molecule, and θ is the angle between $\partial\mu/\partial Q$ and E. The electromagnetic mechanism assumes an increase of the local electric field (E) at the surface of the AgNPs [35,36]. On the other hand, the chemical mechanism assumes an increase of $\left|\partial\mu/\partial Q\right|^2$ (i.e., the absorption coefficient) due to the chemical interactions between the absorbed glucose molecules and the surface of the nanoparticles [37,38]. Therefore, the enhancement of the infrared absorption signal is the collaborative result of both the electromagnetic and chemical mechanisms. However, it is difficult to grow AgNPs on the cylindrical surface of the single-loop fiber ATR sensor. In this paper, a chemical silver mirror method was proposed to grow nanoparticles on the cylindrical surface of the single-loop fiber ATR sensor.

3. Fabrication of AgNPs on cylindrical surface of single-loop fiber ATR sensor

3.1. Growing method of AgNPs by chemical silver mirror

The chemical silver mirror method, one of the wet chemical methods, is simple, highly reproducible and effective in preparing metallic nanoparticles [39,40]. Moreover, it is not limited to flat substrates. In the chemical silver mirror method, glucose acts as a reducing agent to reduce silver ions of $[Ag(NH_3)_2]OH$. The reduction of silver ions is expressed in the following equations:

$$AgNO_3 + NH_3{\cdot}H_2O \rightarrow NH_4NO_3 + AgOH$$

$$2AgOH \rightarrow Ag_2O + H_2O$$

$$Ag_2O + 4NH_3{\cdot}H_2O \rightarrow 2[Ag(NH_3)_2]OH$$

$$CH_2OH(CHO)_4CHO + 2[Ag(NH_3)_2]OH \rightarrow CH_2OH(CHO)_4COONH_4 + 2Ag\downarrow + 3NH_3{\cdot}H_2O \quad (2)$$

As soon as the last step of reaction begins, the fiber ATR sensor was placed into the solution and the Ag element was deposited on the spot of the sensor after the designated reaction time. As glucose and fiber materials are non-reactive, the sensor is only a point of attachment for the silver nanoparticles. The morphologies of the AgNPs could be controlled by varying the reaction conditions and were examined by the scanning electron microscopy (SEM).

3.2. Chemicals

Silver nitrate ($AgNO_3$), ammonia ($NH_3{\cdot}H_2O$) and sodium hydroxide (NaOH) were purchased from Jiangtian Chemical Technology Co., Ltd. (Tianjin, China). Peroxide (H_2O_2), ethanol (C_2H_5OH) and glucose were purchased from Guangfusci Co. (Tianjin, China). The fiber ATR sensors were purchased from A.R.T. Photonics GmbH (Berlin, Germany). All chemicals were of analytical grade. Deionized water was used for the preparation of all aqueous solutions.

3.3. Growing process of AgNPs on single-loop fiber ATR sensors

All of the glassware were cleaned in ethanol, peroxide and deionized water; ultrasonicated for 15 min; and dried (70 °C for 30 min). The ammonia (2%) was added slowly in different concentrations of silver nitrate solution (0.5%, 1%, 1.5% and 2%). The pH value of the solution was measured and adjusted to 10 with a few drops of sodium hydroxide. We then added the glucose (10%) to the silver ammonia solution; the dose of glucose depends on the concentrations of silver nitrate. We put the fiber ATR sensor in the solution. The reaction temperature was controlled by a water bath at 60 °C; when the designated reaction time (30 s, 60 s, 90 s) was finished, the fiber ATR sensor was removed from the solution and soaked in deionized water for 2 min to terminate the reaction. All of the soluble particles were dissolved in deionized water. The SEM observation was performed with an S-4800 microscope (Hitachi, Japan). All of the experimental procedure was processed in a dark room to avoid the degradation of silver halide fiber.

3.4. Effect of different growing conditions on AgNPs

During the process of depositing AgNPs on the cylindrical surface of the fiber ATR sensor, the distribution and the size of AgNPs changed under different conditions and this size will eventually affect the absorption signals of the glucose. The conditions that affect the size are the concentration of silver nitrate and the reaction time. To simplify the description of the system used, the fiber ATR sensor conditions are denoted in the following manner: $P^x t^k$, P represents the concentration of silver nitrate by x%, t represents the reaction time by k second. For example, $P^{1\%}t^{60}$ represents fiber ATR sensor prepared by 1% of silver nitrate in a reaction time of 60 s. The size and distribution of AgNPs grown on the circumference surface of fiber ATR sensor were preliminarily evaluated using scanning electron microscope, and the resulting images are shown in Figs. 3.

(1) Effect of the concentration of silver nitrate.
Comparing Fig. 3A to D, it is clear that the AgNP size is larger when the concentration of silver nitrate is higher, and it is also easier to percolate. With a low concentration of silver nitrate, the silver ions were too small to form the AgNPs. The AgNPs are very small and few when the concentration of silver nitrate is 0.5%, and the size of the AgNPs is 30–40 nm. When the concentration of silver nitrate is increased to 1%, the AgNPs are uniform and the size is approximately 50 nm. When the concentration of silver nitrate is more than 1.5%, the AgNPs begin to aggregate and the size of the AgNPs is 80–150 nm. At that concentration, the AgNPs are percolated, which would not yield as large a glucose absorption signal as the following experimental result would indicate.
(2) Effect of deposition time.

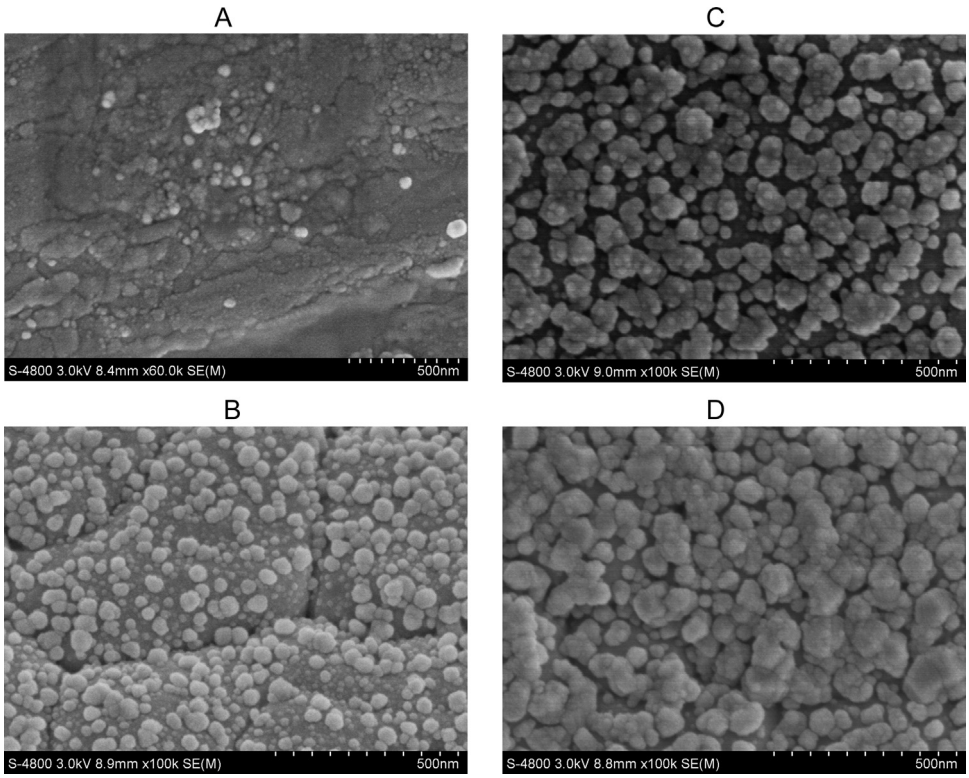

Fig. 3. Effect of concentration of silver nitrate (A) $P^{0.5\%}t^{60}$, (B) $P^{1\%}t^{60}$, (C) $P^{1.5\%}t^{60}$, (D) $P^{2\%}t^{60}$.

Comparing Fig. 4A to C, the size of AgNPs increases as the reaction time of hot water bath increases, and the sizes of the AgNPs are 45 nm, 50 nm and 100 nm when the reaction times in the hot water bath are 30 s, 60 s and 90 s, respectively. We can see that the reaction time of 60 s in the hot water bath is most suitable to grow the AgNPs on the surface, as longer time would lead to clustered AgNPs, which would not yield as large an enhancement as the following experimental results would indicate. During the process of the experiment, adding two drop of ethanol will also make the AgNPs uniform and decrease the percolation.

The absorption bands are distorted to derivative band shapes when the metals are percolated [18]. According to the results of the experiment, the AgNPs are uniform with a size of 50 nm and fewer cluster at the condition of $P^{1\%}t^{60}$. SEM images suggest that a higher concentration of silver nitrate and a longer reaction time would lead the AgNPs to be more easily percolated, which is not favorable for high enhancement; therefore, we choose $P^{1\%}t^{60}$ as the optimal conditions for the growth of the nanoparticles.

3.5. The reproducibility of AgNPs by chemical silver mirror

It is a challenge to control the distribution and the size of AgNPs by chemical deposition method. We carried out a lot of experiments to try to overcome this difficult. Finally, the uniform AgNPs with size of around 50 nm and almost without cluster were obtained under the optimal deposition conditions ($P^{1\%}t^{60}$) by chemical silver mirror method. Fig. 5A and B are the SEM images of the AgNPs on two different silver halide infrared fibers in our experiments. As you can see from Fig. 5, the distribution and size of the AgNPs on the two different fibers are similar which shows the good reproducibility of AgNPs gown by chemical deposition.

4. Characterization of single-loop fiber ATR sensor enhanced by AgNPs

4.1. Experimental system

Due to the operating principle of the CO_2 laser, it is difficult to tune the wavelength and stabilize the line frequency and power simultaneously. But the stability of line frequency and power were important to the accuracy of the glucose measurement in our experiments. In our study, the wavelength tunable CO_2 laser was customized from Access Laser Co. in Washington in USA. The emission wavenumbers were tuned by linear motor to rotate a grating, and the frequency and power of the tuned lines were stabilized using a photoelectric detection feedback system and a piezo actuator to modulate the cavity length [41]. In this study, the CO_2 laser achieved line tuning over the band of 9.19–9.77 μm; five emission wavenumbers around the glucose absorption peaks 1080 and 1035 cm^{-1}, including 1081, 1076, 1051, 1041 and 1037 cm^{-1} were selected as working wavenumbers for glucose specific determination [16]. The five wavenumbers between the two absorption wavenumbers (1035 cm^{-1} and 1080 cm^{-1}) could be tuned randomly in the theory, but after lots of experiment we found that the five wavenumbers (1081, 1076, 1051, 1041 and 1037 cm^{-1}) which we selected can achieve both high stability of line frequency and power simultaneously compared to other wavenumbers. Because water absorption peaks are not near these wavenumbers, water absorption does not affect the measured values at these wavenumbers. All the operations were controlled by a control board with LabVIEW software installed on a computer.

Concentrations of glucose from 5 to 500 mg/dL were used to characterize the fiber ATR sensor with the optimized AgNPs. As shown in Fig. 6, a dual path laser measurement set-up was established for glucose determination using a tunable CO_2 laser and fiber ATR sensor. An infrared attenuator (Model 401, Lasnix, Berg, Germany) was used to attenuate the high power of the laser

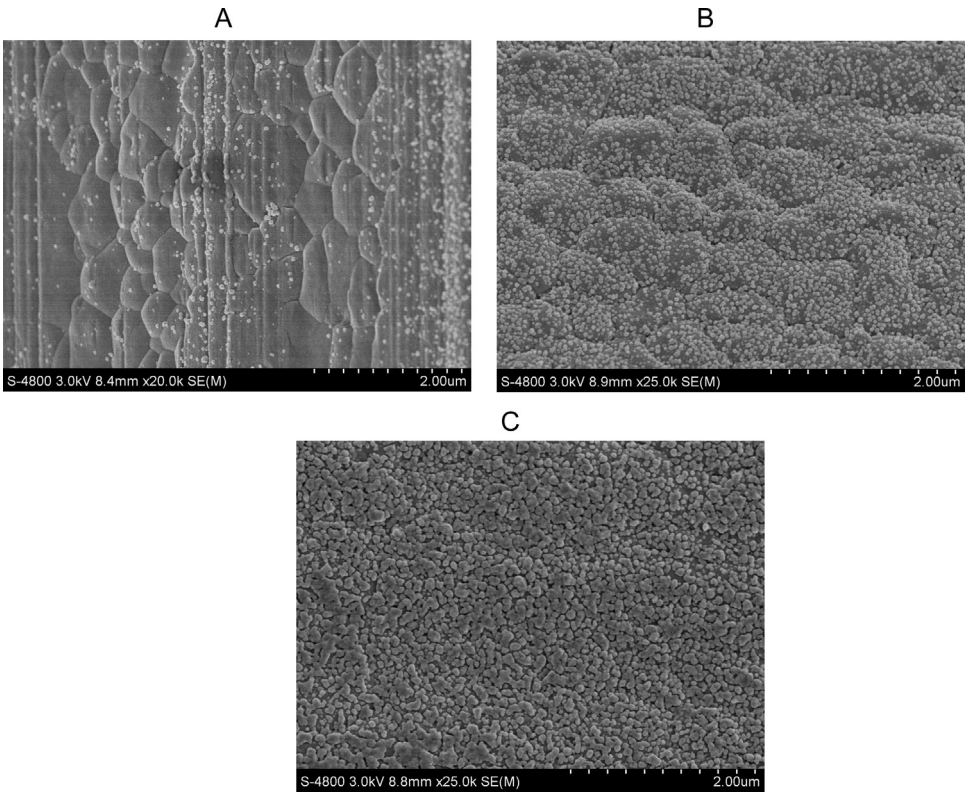

Fig. 4. Effect of deposition time (A) $P^{1\%}t^{30}$, (B) $P^{1\%}t^{60}$, (C) $P^{1\%}t^{90}$.

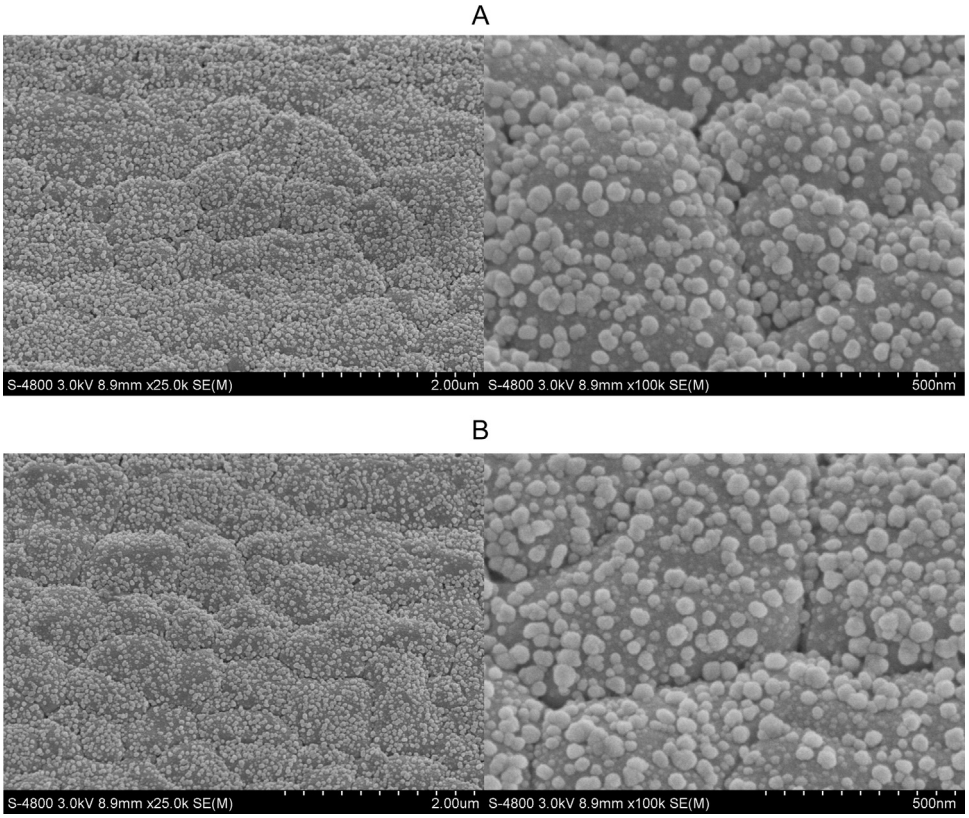

Fig. 5. Morphologies of the AgNPs on two different silver halide infrared fibers.

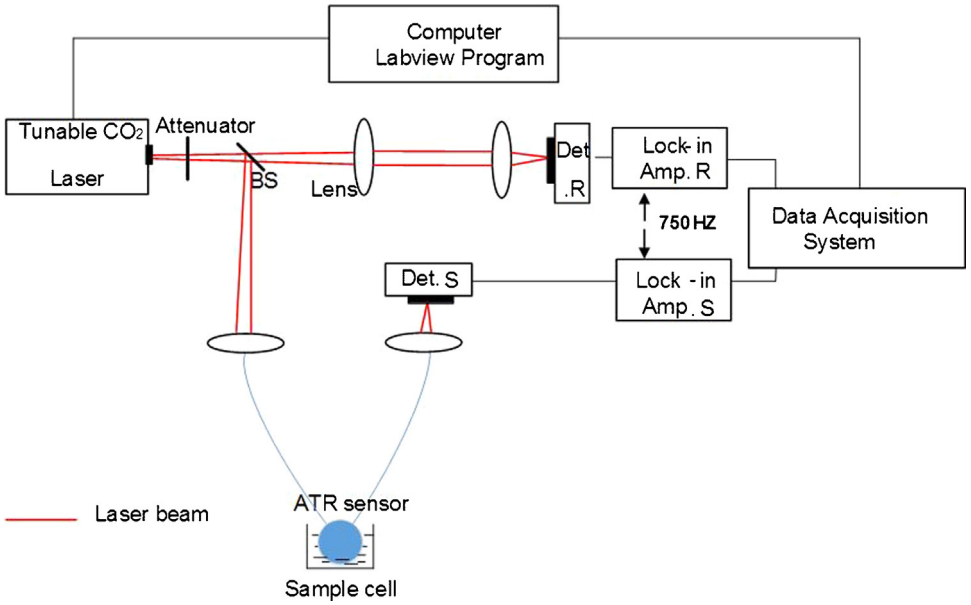

Fig. 6. Schematic of the measurement system of both the bare fiber ATR sensor and the fiber ATR sensor with the optimized AgNPs.

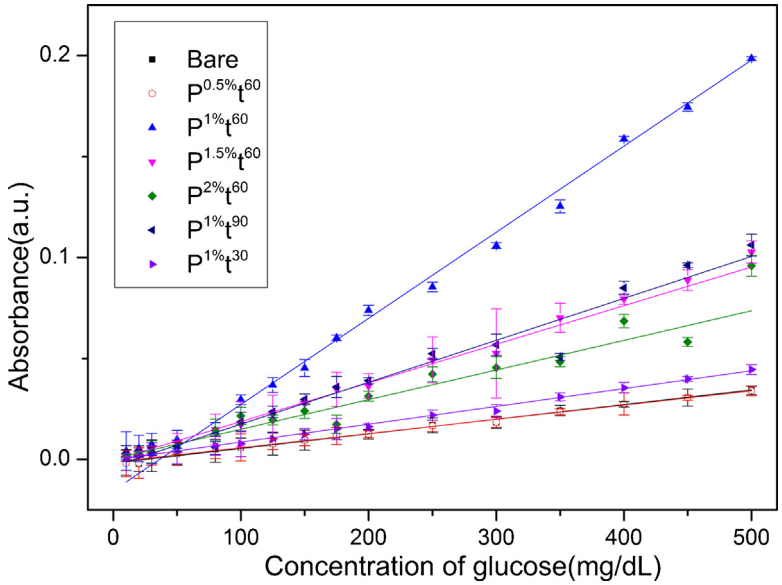

Fig. 7. Plot of absorbance for different single-loop fiber ATR sensors with different nanoparticles.

output to a reasonable level. After being attenuated, the laser beam was divided into dual paths by a Zinc Selenide (ZnSe) beam splitter (BS) for both the reference optic path and sample optic path. Each path's incident laser beam was coupled into the reference and sample detector (Det. R and Det. S) by the ZnSe lens. Two infrared detectors (LME-353, InfraTec GmbH, Dresden, Germany) were matched with two lock-in amplifiers (SR830, Stanford Research Systems, Inc., California, USA). The synchronous reference frequency (750 Hz) was offered by the RF circuit of the laser system. The lock-in signals of the dual paths were then recorded by a data acquisition card synchronously.

The absorbance caused by the change of glucose can be expressed as following equation:

$$A_s = \ln\left(\frac{u_b^s}{u_g^s}\right) + \ln\left(\frac{u_g^r}{u_b^r}\right) \quad (3)$$

where u represents the lock-in amplified voltage, the superscripts "s" and "r" represents the sample and reference paths, respectively, and the subscripts "b" and "g" denote the background and glucose solutions, respectively. A bare fiber ATR sensor was always used as a control. In this experiment, a water solution was employed as both the sample and background solution, and the transmission intensities of the same solution were recorded at the five tuning lengths.

4.2. Effect of different AgNPs for the performance of single-loop fiber ATR sensors

To investigate the characteristic of the fiber ATR sensors enhanced by AgNPs with different growing nanoparticles, a series of different concentrations of glucose ranging from 5 to 500 mg/dL were configured to characterize the enhancement based on the ATR theory. Fig. 7 is a plot of the absorbance for different single-loop

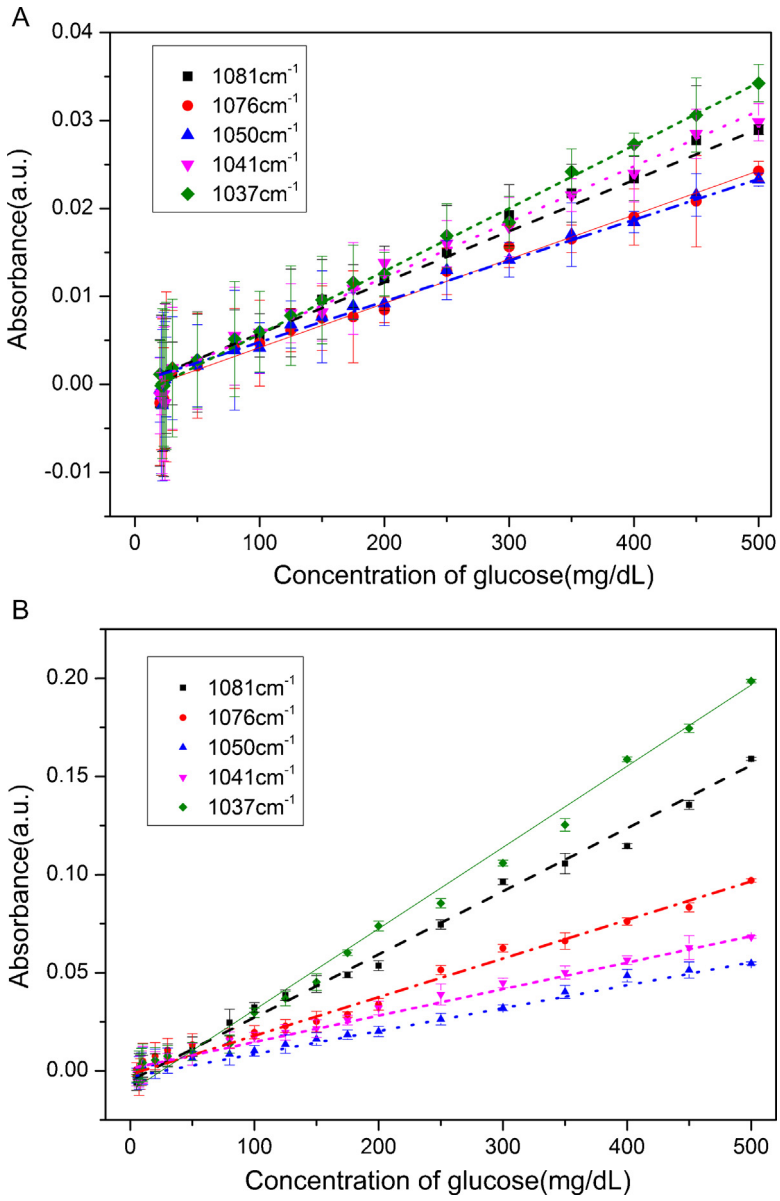

Fig. 8. Plot of absorbance for both the bare fiber ATR sensor (A) and the fiber ATR sensor with the optimized AgNPs (B) at five wavelengths.

fiber ATR sensors with AgNPs grown under different conditions. The absorbance of the glucose based on the single-loop fiber ATR sensors with AgNPs at $P^{0.5\%}t^{60}$ have a little difference compared with the bare ATR sensors. With bigger and denser AgNPs, such as the growing condition of at $P^{1.5\%}t^{60}$ and $P^{1\%}t^{30}$, the sensors have some enhancement compared with the bare one. However, the performance of the sensor decreased when the nanoparticles was percolated such as the growing condition of at $P^{2\%}t^{60}$ and $P^{1\%}t^{90}$, the linearity and the repeatability of the sensor was not very good at the same time. Above all, the growing condition at $P^{1\%}t^{60}$ was considered the optimum condition because it has the best performance in Fig. 7. As the enhancement trends at each of the five wavenumbers are similar, here only the glucose measurement result of one wavenumbers was given.

4.3. Characterization of single-loop fiber ATR sensors with optimized AgNPs

AgNPs were grown on the surface of single-loop fiber ATR sensors under the optimum growing condition at $P^{1\%}t^{60}$. Fig. 8 shows the absorbance of glucose on both the bare fiber ATR sensor and the fiber ATR sensor with the optimized AgNPs at five wavenumbers combined with the set-up of the dual optical path. We can obtain an approximate trend from Fig. 8 and Table 1. The absorbance of glucose at very low concentrations, which have very weak signals, may reach negative values due to the noise of CO_2 laser itself.

If the glucose concentration is altered by δC and the corresponding change in the absorbance of the fiber ATR sensor is δA, then the sensitivity of the fiber ATR sensor could be defined as(4)$S_n = \frac{\delta A}{\delta C}$

The enhancement factor is defined as the ratio of the sensitivity of as-deposited AgNPs fiber ATR sensor to the sensitivity of the bare fiber ATR sensor. As seen in Fig. 2, the absorbance of glucose was different at different wavenumbers. According to Lambert–Beer's Law, under the wavenumber with strong absorbance, the change in glucose concentration will bring larger change of the absorbance. Therefore, the sensitivity depends on the wavenumbers. Five wavenumbers around two strong absorption peaks of glucose ($1035\,cm^{-1}$ and $1080\,cm^{-1}$) were selected to achieve high sensitivity and we didn't choose the five wavenumbers between another

Table 1
Characterization of single-loop fiber ATR sensors with AgNPs.

Bare/AgNPs	Wavenumbers (cm^{-1})				
	1081	1076	1051	1041	1037
S	6.44E−5/3.10E−4	5.14E−5/1.90E−4	4.99E−5/1.14E−4	6.53E−5/1.41E−4	7.02E−5/3.95E−4
R^2	0.987/0.995	0.982/0.989	0.983/0.988	0.985/0.990	0.997/0.992
DL(mg/dL)	24/7	24/9	23/8	25/8	24/7

S: The slope of the straight line in Fig. 8 and the sensitivity of the fiber ATR sensor. R^2: The linearity of the line at each wavenumbers. DL: The detection limit of the fiber ATR sensor.

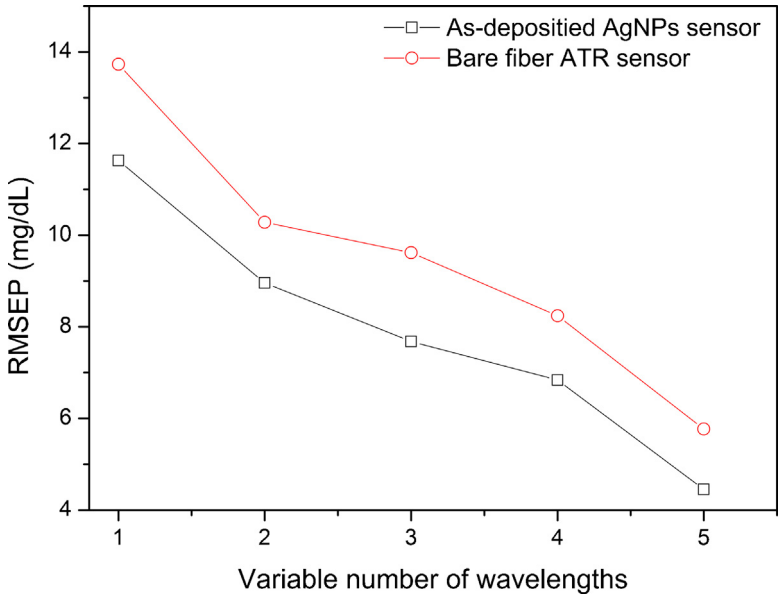

Fig. 9. Plot of the RMSEP value against the number of wavelengths by cross-validation PLS model.

two glucose absorption wavenumbers such as 1107 cm^{-1} and 1152 cm^{-1}.

From the table, we obtain three types of information: (1) The fiber ATR sensor with the optimized AgNPs improved the sensitivity at different wavenumbers (1081, 1076, 1051, 1041 and 1037 cm^{-1}) compared with the bare fiber ATR sensor. The estimated enhancement factors at each of the five wavenumbers (1081, 1076, 1051, 1041 and 1037 cm^{-1}) were 4.81, 3.70, 2.28, 2.16 and 5.63, respectively. These values were determined by calculating the sensitivity of fiber ATR sensors. (2) The linearity of the as-deposited AgNPs fiber ATR sensor is as good as the bare fiber ATR sensor. Linearity of both types of fiber ATR sensors are better than $R^2 \geq 0.98$. (3) Glucose solution with different concentrations from 5 to 40 mg/dL with 1 mg/dL intervals was used to characterize the detection limit of the bare fiber ATR sensor and the fiber ATR sensor with the AgNPs by experiments. And the detection limit for glucose of the fiber ATR sensor was changed from 23 to 7 mg/dL by growing the AgNPs on the surface of the fiber, which means that the measurement resolution of the fiber ATR sensor is greatly improved. All of above could confirm that the as-deposited AgNPs fiber ATR sensor shows a higher enhancement capacity at the optimal condition by chemical silver mirror method than conventional measurements.

4.4. Evaluation of fiber ATR sensor for glucose measurement

The calibration was carried out by a partial least-squares (PLS) algorithm with spectral data from the five wavelengths, and a cross-validation was performed to optimize the PLS model. According to the spectral analysis, a single wavelength is not enough to determine one analyte using a discrete wavelength spectrometer. At least 3–5 working wavelengths are needed for the stability of the prediction mode to determine one analyte. The prediction quality of the PLS mode was compared for various variable wavelength numbers using the root-mean-square error of prediction (RMSEP). Fig. 9 shows that the RMSEP decreases sharply with the increasing wavelengths by cross-validation of the PLS model. The best performance of the ATR sensor enhanced by AgNPs was achieved with the five-wavelength PLS model yielding a RMSEP that was smaller than the bare fiber ATR sensor. The best prediction of glucose concentration was achieved using the five-variable partial least-squares model yielding a root-mean-square error of prediction as small as 4.45 mg/dL based on the as-deposited AgNPs fiber ATR sensor, which is clinically acceptable [30].

5. Conclusion

In this study, we proposed a miniaturized implantable fiber ATR sensor for continuous glucose determination that could reduce the signal drift and overcome the difficulty of hypoglycemia detection compared with the enzyme electrode sensing technique. A single-loop structure was used to increase the effective optical length to enhance the sensitivity of the optical ATR sensor. AgNPs were grown on the cylindrical surface of the single-loop fiber ATR sensor by the chemical silver mirror method to further improve the measurement resolution. A dual optical laser measurement setup was presented to characterize the ATR sensor enhanced by AgNPs and bare fiber ATR sensor by measuring the concentrations of glucose. Experimental results show that the ATR sensor enhanced by AgNPs at the optimum condition possessed a better sensitivity compared with the bare fiber ATR sensor, with an enhancement factor between 2 and 6 times at different glucose absorption wavenumbers. The detection limit of the ATR sensor

enhanced by AgNPs was as low as 7 mg/dL, which is suitable for continuous glucose monitoring in clinical applications. A multivariable partial least-squares model was used to calibrate the spectral data for the five wavenumbers, which shows the advantage of as-deposited AgNPs sensor over the bare ATR sensor. The proposed fiber ATR sensor has already been miniaturized in our study for implantable application. But the fiber ATR sensor needs to be connected to a spectrometer out of body to process the data. The spectrometer is still a little bigger. However, the miniaturization of spectrometer is ongoing and it is also a hot research field in recent years. The instrument of ATR glucose sensing will become portable soon with miniaturized fiber ATR sensor and miniaturized spectrometer together for long time continuous glucose monitoring in the near future. Therefore, future studies will further investigate the biocompatible encapsulation of the fiber ATR sensor using biological materials through animal experiments.

Acknowledgments

This work was supported by the National Natural Science Foundation of China (no. 61176107, no. 51350110233, no. 11204210, no. 61428402 and no. 61201039), the Key Program of Tianjin Natural Science Foundation (no. 15JCZDJC36100), the National Key Projects in Non-profit Industry (no. GYHY200906037), the National High Technology Research and Development Program of China (no. 2012AA022602), and the 111 Project of China (no. B07014).

References

[1] Continuous Glucose Monitoring: Innovation in the Management of Diabetes, Report of New England Healthcare Institute, 2002.
[2] C. Zecchin, A. Facchinetti, G. Sparacino, A new neural network approach for short-term glucose prediction using continuous glucose monitoring time-series and meal information, in: Conf. Proc. IEEE Eng. Med. Biol. Soc., 2011, pp. 5653–5656.
[3] Y.J. Lee, J.D. Kim, J.Y. Park, Flexible enzyme free glucose micro-sensor for continuous monitoring applications, in: Solid-State Sensors, Actuators and Microsystems Conference, 2009, pp. 1806–1809.
[4] K.W. Cooper, G. Soundararajan, J.B. Sanders, et al., Clinical experience with an integrated continuous glucose sensor-insulin pump platform: a feasibility study, Advances in Therapy 23 (5) (2006) 725–732.
[5] J. Mastrototaro, J. Shin, A. Marcus, et al., The accuracy and efficacy of real-time continuous glucose monitoring sensor in patients with type 1 diabetes, Diabetes Technology & Therapeutics 10 (5) (2008) 385–390.
[6] R.L. Weinstein, S.L. Schwartz, R.L. Brazg, et al., Accuracy of the 5-day FreeStyle Navigator continuous glucose monitoring system comparison with frequent laboratory reference measurements, Diabetes Care 30 (5) (2007) 1125–1130.
[7] D.M. Wilson, R.W. Beck, W.V. Tamborlane, et al., The accuracy of the FreeStyle Navigator continuous glucose monitoring system in children with type 1 diabetes, Diabetes Care 30 (1) (2007) 59–64.
[8] R. Safavieh, et al., Straight SU-8 pins, Journal of Micromechanics and Microengineering 20 (2010) 055001.
[9] D.B. Keenan, R. Cartaya, J.J. Mastrototaro, Accuracy of a new real-time continuous glucose monitoring algorithm, Journal of Diabetes Science and Technology 4 (1) (2010) 111–118.
[10] B. Kovatchev, S. Anderson, L. Heinemann, et al., Comparison of the numerical and clinical accuracy of four continuous glucose monitors, Diabetes Care 31 (6) (2008) 1160–1164.
[11] T. Bailey, H. Zisser, A. Chang, New features and performance of a next-generation SEVEN-day continuous glucose monitoring system with short lag time, Diabetes Technology & Therapeutics 11 (12) (2009) 749–755.
[12] S.S. Kim, C. Young, B. Mizaikoff, Miniaturized mid-infrared sensor technologies, Analytical and Bioanalytical Chemistry 390 (1) (2008) 231–237.
[13] C.B. Minnich, L. Kuepper, M.A. Liauw, et al., Combining reaction calorimetry and ATR-IR spectroscopy for the *operando* monitoring of ionic liquids synthesis, Catalysis Today 126 (1) (2007) 191–195.
[14] P. Polynkin, A. Polynkin, N. Peyghambarian, et al., Evanescent field-based optical fiber sensing device for measuring the refractive index of liquids in microfluidic channels, Optics Letters 30 (11) (2005) 1273–1275.
[15] Y. Cao, W. Zhang, R. Liu, et al., Study of specificity for noninvasive glucose measurements based on two-dimensional correlation mid-infrared spectroscopy, in: SPIE BiOS, International Society for Optics and Photonics, 2012, pp. 82291B–82291B-11.
[16] S. Yu, D. Li, H. Chong, et al., In vitro glucose measurement using tunable mid-infrared laser spectroscopy combined with fiber-optic sensor, Biomedical Optics Express 5 (1) (2014) 275–286.
[17] Chen Lu, Xing Bo Liang, Yang Liu, Study of influencing factors on vacuum evaporation film thickness, Applied Mechanics and Materials 543 (2014) 3716–3720.
[18] N. Khedmi, M. Ben Rabeh, M. Kanzari, Structural morphological and optical properties of $SnSb_2 S_4$ thin films grown by vacuum evaporation method, Journal of Materials Science & Technology 30 (10) (2014) 1006–1011.
[19] F. Verger, T. Pain, V. Nazabal, et al., Surface enhanced infrared absorption (SEIRA) spectroscopy using gold nanoparticles on $As_2 S_3$ glass, Procedia Engineering 25 (2011) 1645–1648.
[20] J.M. Delgado, J.M. Orts, J.M. Pérez, et al., Sputtered thin-film gold electrodes for in situ ATR-SEIRAS and SERS studies, Journal of Electroanalytical Chemistry 617 (2) (2008) 130–140.
[21] Á.I. López-Lorente, M. Sieger, M. Valcarcel, et al., Infrared attenuated total reflection spectroscopy for the characterization of gold nanoparticles in solution, Analytical Chemistry 86 (1) (2013) 783–789.
[22] G.P.C. Rao, J. Yang, Preparation of high-capacity substrates from polycrystalline silver chloride for the selective detection of tyrosine by surface-enhanced infrared absorption (SEIRA) measurements, Analytical and Bioanalytical Chemistry 401 (9) (2011) 2935–2943.
[23] R.L.J. Chang, J. Yang, Surface-controlled electroless deposition method in the preparation of stacked silver nanoparticles on germanium for surface-enhanced infrared absorption measurements, Applied Spectroscopy 64 (2) (2010) 211–218.
[24] Á.I. López-Lorente, M. Sieger, M. Valcarcel, et al., Infrared attenuated total reflection spectroscopy for the characterization of gold nanoparticles in solution, Analytical Chemistry 86 (1) (2013) 783–789.
[25] A. Pasic, H. Koehler, I. Klimant, et al., Miniaturized fiber-optic hybrid sensor for continuous glucose monitoring in subcutaneous tissue, Sensors and Actuators B: Chemical 122 (1) (2007) 60–68.
[26] X. Huang, S. Li, J.S. Schultz, et al., A MEMS affinity glucose sensor using a biocompatible glucose-responsive polymer, Sensors and Actuators B: Chemical 140 (2) (2009) 603–609.
[27] M. Pleitez, H. von Lilienfeld-Toal, W. Mäntele, Infrared spectroscopic analysis of human interstitial fluid in vitro and in vivo using FT-IR spectroscopy and pulsed quantum cascade lasers (QCL): establishing a new approach to noninvasive glucose measurement, Spectrochimica Acta Part A: Molecular and Biomolecular Spectroscopy 85 (1) (2012) 61–65.
[28] U. Damm, V.R. Kondepati, H.M. Heise, Continuous reagent-free bed-side monitoring of glucose in biofluids using infrared spectrometry and micro-dialysis, Vibrational Spectroscopy 43 (1) (2007) 184–192.
[29] H.M. Heise, G. Voigt, P. Lampen, et al., Multivariate calibration for the determination of analytes in urine using mid-infrared attenuated total reflection spectroscopy, Applied Spectroscopy 55 (4) (2001) 434–443.
[30] S. Yu, D. Li, H. Chong, et al., Continuous glucose determination using fiber-based tunable mid-infrared laser spectroscopy, Optics and Lasers in Engineering 58 (2014) 78–83.
[31] F. Moser, N. Barkay, A. Levite, et al., Research and development on silver halide fibers at Tel Aviv University, Proceedings of SPIE 1228 (1990) 128–139.
[32] A. Sa'Ar, N. Barkay, F. Moser, et al., Optical and mechanical properties of silver halide fibers, in: OE/Fibers' 87, International Society for Optics and Photonics, 1987, pp. 98–104.
[33] M. Saito, M. Takizawa, M. Miyagi, Optical and mechanical properties of infrared fibers, Journal of Lightwave Technology 6 (2) (1988) 233–239.
[34] M. Osawa, Surface-enhanced infrared absorption, in: Near-Field Optics and Surface Plasmon Polaritons, Springer, Berlin/Heidelberg, 2001, pp. 163–187.
[35] A. Hartstein, J.R. Kirtley, J.C. Tsang, Enhancement of the infrared absorption from molecular monolayers with thin metal overlayers, Physical Review Letters 45 (3) (1980) 201.
[36] M. Osawa, Dynamic processes in electrochemical reactions studied by surface-enhanced infrared absorption spectroscopy (SEIRAS), Bulletin of the Chemical Society of Japan 70 (12) (1997) 2861–2880.
[37] G.T. Merklin, P.R. Griffiths, Influence of chemical interactions on the surface-enhanced infrared absorption spectrometry of nitrophenols on copper and silver films, Langmuir 13 (23) (1997) 6159–6163.
[38] P. Dumas, R.G. Tobin, P.L. Richards, Study of adsorption states and interactions of CO on evaporated noble metal surfaces by infrared absorption spectroscopy: II. Gold and copper, Surface Science 171 (3) (1986) 579–599.
[39] B. Schweig, Mirrors: A Guide to the Manufacture of Mirrors and Reflecting Surfaces, Pelham Books, London, 1973.
[40] H. Lilienfeld-Toal von, M. Weidenmülle, A. Xhelaj, et al., Vibrational Spectroscopy 38 (2005), 209–215.
[41] S. Yu, D. Li, H. Chong, et al., In vitro glucose measurement using tunable mid-infrared laser spectroscopy combined with fiber-optic sensor, Biomedical Optics Express 5 (1) (2014) 275–286.

Biographies

Dachao Li received a B.S. degree in precision instruments from Tianjin University, Tianjin, China, in 1998 and M.S. and Ph.D. degrees in precision instruments and mechanics from Tianjin University, Tianjin, China, in 2001 and 2004, respectively. Li was previously a research associate at the Department of Electrical Engineering and Computer Science, Case Western Reserve University, Cleveland, Ohio, USA (2006–2008). Currently, he is a professor in the College of Precision Instruments and Optoelectronics Engineering, Tianjin University. His research interests focus on micro-sensors and opto-fluidics.

Yanwen Sun received his bachelor's degree in 2012 from the Zhengzhou University of Light Industry, Henan, China. Currently, he is studying his master's degree at the Tianjin University, Tianjin, China. His research work is concentrated on fiber-optic ATR sensors for glucose measurement.

Songlin Yu received his doctoral degree in 2014 from Tianjin University, Tianjin, China. His research focus on glucose measurement using tunable laser spectroscopy combined with fiber-optic ATR sensors.

Changyue Sun received her bachelor's degree in 2012 from the Changchun University of Science and Technology, Jilin, China. Currently, she is completing her master's degree at the Tianjin University, Tianjin, China. Her research work is concentrated on fiber-optic ATR sensors for glucose measurement.

Haixia Yu received her doctoral degree in 2011 from Tianjin University, Tianjin, China. Currently, she is an associate professor in the College of Precision Instruments and Optoelectronics Engineering, Tianjin University. Her research interests focus on biomedical microfluidics and biomedical micro-sensors.

Kexin Xu received his B.S. degree in precision instrument engineering from Harbin University of Science and Technology, Harbin, China, in 1982 and his Ph.D. degree in precision instrument engineering from Tianjin University, Tianjin, China, in 1988. He has been a professor full-time professor and researcher in the College of Precision Instrument and Optoelectronics Engineering, Tianjin University. His research interests include the design theory of acousto-optic tunable filter and spectroscopic technology, rapid detection of milk ingredients, monitoring of air and flue gas composition and non-invasive glucose monitoring.